Journal of Oleo Science
Copyright ©2020 by Japan Oil Chemists' Society
J-STAGE Advance Publication date : September 10, 2020
doi : 10.5650/jos.ess20113
J. Oleo Sci.

Actuation Properties of Paper Actuators Fabricated Using PEDOT/PSS Electrode Films

Yujiao Wu[1, 2], Hiroyuki Minamikawa[1]*, Tomoka Nakazumi[1], and Yusuke Hara[1, 2]*

[1] *Research Institute for Sustainable Chemistry, National Institute of Advanced Industrial Science and Technology (AIST), Central 5, 1-1-1 Higashi, Tsukuba, Ibaraki 305-8565, JAPAN*

[2] *Department of Nano-science and Nano-Technology, Graduate School of Pure and Applied Sciences, University of Tsukuba, Tsukuba, Ibaraki 305-8571, JAPAN*

Abstract: The development of actuators for power sources is essential for the efficient manipulation of fluids in microfluidics systems. In this work, a capacitor-type three-layer paper actuator was fabricated by sandwiching a polyelectrolyte layer between two films of poly(3,4-ethylenedioxythiophene) doped with poly(4-styrenesulfonate) (PEDOT/PSS). The paper actuator exhibited stable large electromechanical deformations in bilateral symmetry under alternating square-wave electric field. The actuation properties were examined in a function of voltage (±0.5, ±1, ±1.5, ±2, and ±2.5 V) and frequency (1, 0.5, 0.2, and 0.05 Hz). In addition, the PEDOT/PSS electrode films with different thicknesses were prepared, and the effects of actuator thickness on actuation properties were examined. As a result, it was found that the actuator displacement increased considerably with reducing actuator thickness. In addition, the actuator with a thickness of 48 μm demonstrated a maximum displacement of 5.8 mm at a voltage of 1.5 V and frequency of 0.05 Hz. The proposed actuator can be potentially used in the development of power sources for micropumps and check valves of microfluidic devices.

Key words: PEDOT/PSS electrode, paper actuator, actuation properties, bending deformation, actuator thickness

1 Introduction

Microfluidics technology has attracted significant attention owing to its ability to manipulate small quantities of fluids by using microchannels. Recently microfluidics technology has been utilized for microdroplet dispersion technology which can generate monodisperse emulsions for the food processing, pharmaceutical, cosmetics, and chemical applications[1)]. Microfluidics technology is also applicable to separate/detect continuous various size particles (particle classification) through microchannel geometries with high resolutions and sensitivities[2)]. In addition, the recent advances in microfluidics led to the development of DNA chip[3)], lab-on-a-chip (LOC)[4)], and micro-propulsion[5)] technologies. LOC is promising application of microfluidics devices that integrates one or multiple laboratory functions scaled to a chip format to perform multiplexing analysis, automation, and high-throughput screening. LOC devices are portable and considerably reduce the apparatus operational footprints of analytical and diagnostic systems as compared with those of the conventional machines. LOCs containing microchannels have been applied in chemical reactions[6)], biological pathogen detection[7, 8)], and medicinal diagnostics including point-of-care testing (POCT)[9, 10)] that allows immediately conducting simple diagnostic tests in a relatively short therapeutic time, which improves the patient care quality and clinical outcomes and reduces patient suffering.

In microfluidics systems, the use of efficient power sources for micropumps and check valves is essential for realizing precise control and on-demand release of fluids. In previous works, pumps and valves were controlled by pneumatic[11)], hydraulic[11)], piezoelectric[12, 13)], electromagnetic[14, 15)], and electroactive polymer (EAP) actuators[16, 17)]. Among these devices, EAP actuators are widely utilized in microelectromechanical systems (MEMS) and micrototal analysis systems (μTAS) because of their softness, flexibility, low weight, and ability to be easily trimmed for miniaturization. The EAP actuators that easily change their sizes or shapes under the action of electric fields can be categorized into electronic and ionic EAPs. However, electronic EAP actuators require a high driving voltage, which is not desirable for microfluidic application. In contrast, ionic EAP actuators undergo large electromechanical deformations because of the ion migration that occurs at low

*Correspondence to: Yusuke Hara and Hiroyuki Minamikawa, Research Institute for Sustainable Chemistry, National Institute of Advanced Industrial Science and Technology (AIST), Central 5, 1-1-1 Higashi, Tsukuba, Ibaraki 305-8565, JAPAN
E-mail: y-hara@aist.go.jp (Y. H.); hiroyuki.minamikawa@aist.go.jp (H. M.)
Accepted June 5, 2020 (received for review April 24, 2020)
Journal of Oleo Science ISSN 1345-8957 print / ISSN 1347-3352 online
http://www.jstage.jst.go.jp/browse/jos/ http://mc.manusriptcentral.com/jjocs

driving voltages (1 − 5 V)[18, 19]. As a typical example, the ionic polymer-metal composites (IPMCs) developed for microfluidic pumps and valves[16, 17] exhibit large bending displacements at low voltages[20, 21]. However, they also have several drawbacks. Although IPMCs contain Nafion ion-exchange membranes with high proton conductivities and chemical stabilities, the relatively high costs of these materials significantly limit their practical applications. Moreover, the Pt metal electrodes of IPMCs exhibit poor adhesions to the ion-exchange membranes and require a time-consuming manufacturing process by chemical plating, while their electrode surfaces can be easily damaged. Therefore, it is imperative to develop alternative soft materials for microfluidic actuators.

In a previous work, we developed a novel paper actuator fabricated using ionic EAPs by sandwiching a polyelectrolyte layer between two films of poly (3,4-ethylenedioxythiophene) doped with poly (4-styrenesulfonate) (PEDOT/PSS) that possessed high stability and electrical conductivity[22]. Compared with the chemically plated Pt electrodes of IPMCs[23] (whose preparation involves chemical reduction of platinum salts such as $Pt(NH_3)_4HCl$), PEDOT/PSS flexible electrodes can be produced by a casting process, which reduces their costs and increases the manufacturing efficiency. Moreover, PEDOT/PSS electrodes possess good adhesion properties because of their electrostatic interactions with the polyelectrolyte layer. Finally, the paper actuator fabricated using PEDOT/PSS electrode films is relatively thin, lightweight, inexpensive, is functional in water, durable, and environmentally friendly[22−25]. Therefore, PEDOT/PSS actuators can be potentially used in the power sources for micropumps or microfluidic valves.

In this study, the preparation process of PEDOT/PSS films was modified to enhance the performance of paper actuators, and their thermal stabilities were determined. To examine the influence of the thickness of a paper actuator on its actuation properties at applied alternating electric field (0.5 − 2.5 V and 0.05 − 1 Hz), actuators with thicknesses of 20 − 95 μm were fabricated. Finally, reproducibility of the measured actuator displacements was demonstrated.

2 Experimental

2.1 Materials

Poly (3,4-ethylenedioxythiophene)/poly (styrene sulfonate) (PEDOT/PSS, high-conductivity grade, 3.3 wt.% aqueous dispersion) was purchased from Sigma-Aldrich. Poly (diallyldimethylammonium chloride) solution (average $M_W = 4 - 5 \times 10^5$, 20 wt.% in H_2O) utilized as a polyelectrolyte layer was also obtained from Sigma-Aldrich. Polyethylene glycol monooleyl ether (PEGM, approximately 20 ethylene glycol units, Tokyo Chemical Industry Co. Ltd., Tokyo, Japan) was used as a surfactant additive.

2.2 Preparation of paper actuators with PEDOT/PSS films

An aqueous PEDOT/PSS solution containing 1 wt.% PEGM was stirred at 200 rpm for 2 h during degassing and then kept under vacuum overnight (the degassing procedure effectively suppressed the formation of bubble-like defects in the film. After that, the polymer solution was poured into a polytetrafluoroethylene (PTFE) petri dish (inner diameter: 30 mm) and dried first at 60℃ for 12 h and then at 120℃ for 3 h. The prepared PEDOT/PSS film was subsequently peeled off from the PTFE petri dish surface with tweezers, as shown in Fig. 1a.

Figure 1b illustrates the fabrication of the paper actuator using PEDOT/PSS films. The structure of the PEDOT/PSS soft actuator is similar to that of the electric-double-layer capacitor. Here, the middle layer represents a polyelectrolyte layer of poly (diallyldimethylammonium chloride) solution that contains movable chloride ions. This solution was cast on the prepared PEDOT/PSS film using a spin coater (1H-D7, Mikasa Co. Ltd., Tokyo, Japan) at 3000 rpm in 10 s. Afterwards, another PEDOT/PSS film was placed on the polyelectrolyte-cast film to form a three-layer actuator structure. The fabricated PEDOT/PSS paper actuator was cut to obtain a rectangular strip 20 mm long and 3.5 mm wide. Two copper electrodes were used as the metal electrodes.

Table 1 lists the weights of the utilized PEDOT/PSS solutions and the thicknesses of the prepared electrode films and fabricated actuators.

2.3 Electromechanical tests

To determine the electro-mechanical deformations of the produced actuators, activating voltages were applied to them. In this experiment, an actuator was fixed to a beam by clipping its upper end with a length of 2.5 mm. The working actuator length was 17.5 mm. The copper electrodes were clipped by Kelvin clips that connected the device to the counter electrodes of a potentiostat (HAL-3001, Hokuto Denko Co. Ltd., Tokyo, Japan). Alternating square-wave voltages (±0.5, ±1, ±1.5, ±2, and ±2.5 V) were applied to the actuator strip, and their frequencies (1, 0.5, 0.2, or 0.05 Hz) were controlled by a function generator (HB-305, Hokuto Denko Co. Ltd., Tokyo, Japan). Simultaneously, electro-mechanical deformation of the tested actuator was recorded by using a digital video camera (30 frames per second). The actuator deflection was measured using ImageJ software.

In this system, water was required for operating the actuator because the solvent is needed to move the chloride ions across the polyelectrolyte layer. Therefore, prior to assessment, the actuator was soaked in water, and the excess water was wiped away. In each actuation experiment, 12

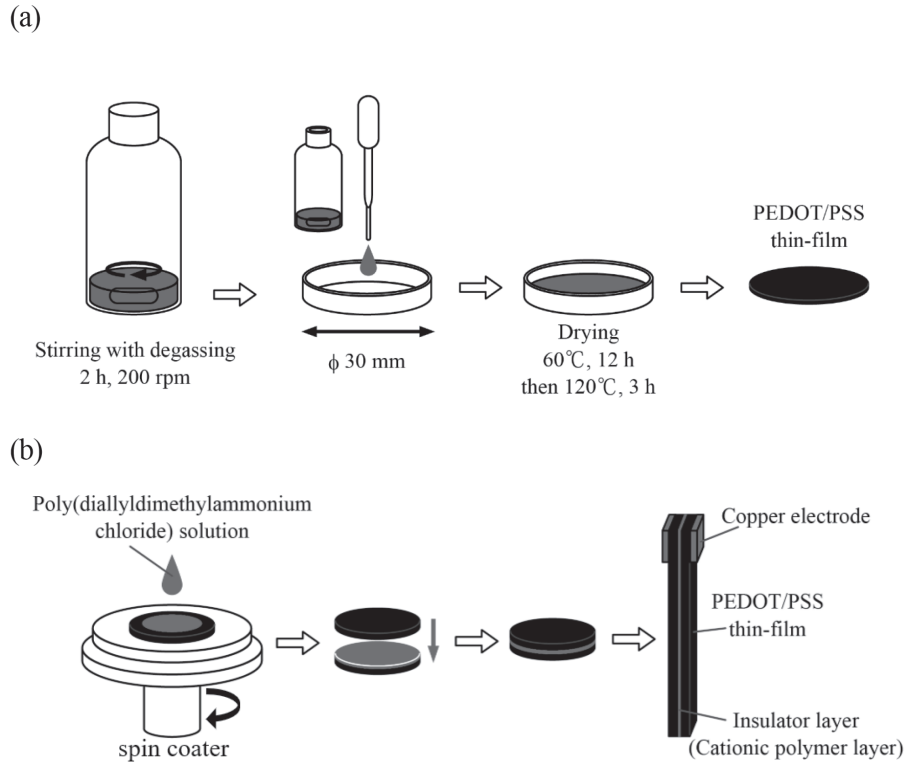

Fig. 1 Fabrication of the paper actuator using PEDOT/PSS films. (a) Preparation of the PEDOT/PSS electrode film. (b) Schematic illustration of the paper actuator (20 mm long, 3.5 mm wide) fabricated by sandwiching a polyelectrolyte layer between two PEDOT/PSS electrode films.

Table 1 Weight of the PEDOT/PSS solution in the petri dish with a diameter of 30 mm and thicknesses of the fabricated electrode films and corresponding actuators.

3.3 wt% PEDOT/PSS solution with 1 wt.% PEGM (g)	Electrode film thickness (μm)	Actuator thickness (μm)
0.6	20	48
0.7	25	55
1.0	33	72
1.3	46	105
1.5	62	135
2.0	95	195

cycles were performed at different applied voltages and frequencies, and the average actuator displacement was estimated from the results obtained from the third to eighth cycles.

3 Results and Discussion

3.1 Thermal stability of PEDOT/PSS films

During the electrode film preparation, the PEDOT/PSS solution was dried at 120℃ for 3 h because very high process temperatures could damage/decompose the chemical structure of the polymer material. The thermal stability of the PEDOT/PSS film was accessed by thermogravimetric analysis (TGA, 6200-S, Seiko Instruments Inc., Chiba, Japan). In this experiment, the film was heated from 25 to 400℃ at a heating rate of 10℃/min under nitrogen gas flow. As shown in Fig. 2, the first weight loss observed below 150℃ is due to water evaporation, while the second significant weight loss that occurred between 200 and 400℃ is attributed to the decomposition of the PEDOT/PSS polymers. These results indicated that the utilized drying conditions did not cause any noticeable chemical decomposition of the prepared PEDOT/PSS film.

3.2 Actuation properties of paper actuators

The actuation properties of the fabricated paper actuators were evaluated by applying alternating square-wave voltages (see Fig. 3a).

Figure 3b shows the deformations of the paper actuator with a thickness of 48 μm at an applied alternating square-wave voltage of ±1.5 V and frequency of 0.05 Hz. Their magnitudes were relatively high, and the actuator was notably bent under the specified conditions.

In Fig. 3c, actuator displacements are plotted as functions of the applied voltage (0.5 to 2.5 V). At a constant

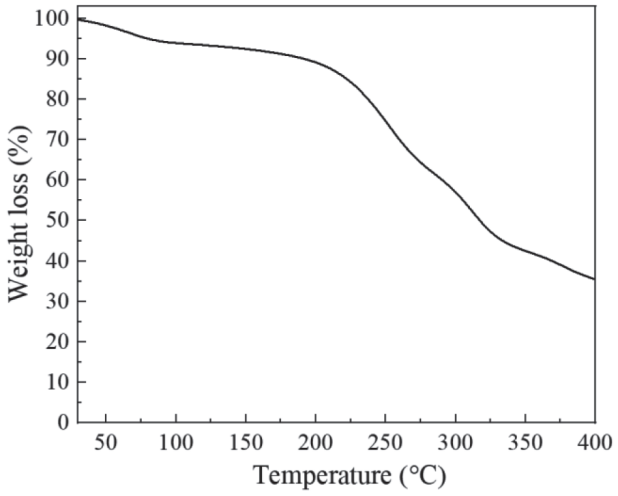

Fig. 2 A TGA curve recorded for the film prepared from the 3.3 wt.% PEDOT/PSS solution containing 1 wt.% PEGM.

frequency of 1 Hz (squares), a small displacement of 1.3 mm was observed at 0.5 V. As the voltage increased to 2.5 V, the displacement increased to 3.2 mm, which could be explained in terms of the voltage-dependent degree of charging a capacitor-type actuator (Fig. 3a). The higher voltages applied to the capacitor effectively increase the chloride anion differential on the anode. The increased chloride ion content on the anode side produces an osmotic pressure differential, which effectively increases the water content in the anode side. Subsequently, the anode side swells, leading to the actuator deflection toward the cathode side.

Similar increases in the actuator displacement were observed with the voltage increase up to 2.0 V at 0.5 Hz (triangles) and to 1.5 V at 0.2 and 0.05 Hz (open diamonds and open circles, respectively). However, during these measurements, the actuator displacement decreased at 2.0 V and 2.5 V, owing to increased Joule heating at higher voltages. The increased Joule heating promotes water evaporation from the paper actuator, which hardens the wet polymer-based device and deteriorates its actuation properties. The displacement drop was particularly large at frequencies of 0.05 and 0.2 Hz, which was likely caused by an increase in the water evaporation effect during the longer operation time at lower frequencies. Indeed, the total operation times (eight cycles) at 1, 0.5, 0.2, and 0.05 Hz were 8, 16, 40, and 160 s, respectively (note that each displacement depicted in Fig. 3c is the average value calculated from the third to eighth cycles). It appears that the longer operation time results in the increased water evaporation, leading to hardening of the device.

3.3 Effect of actuator thickness on deflection

As shown in Table 1, six paper actuators with thickness-

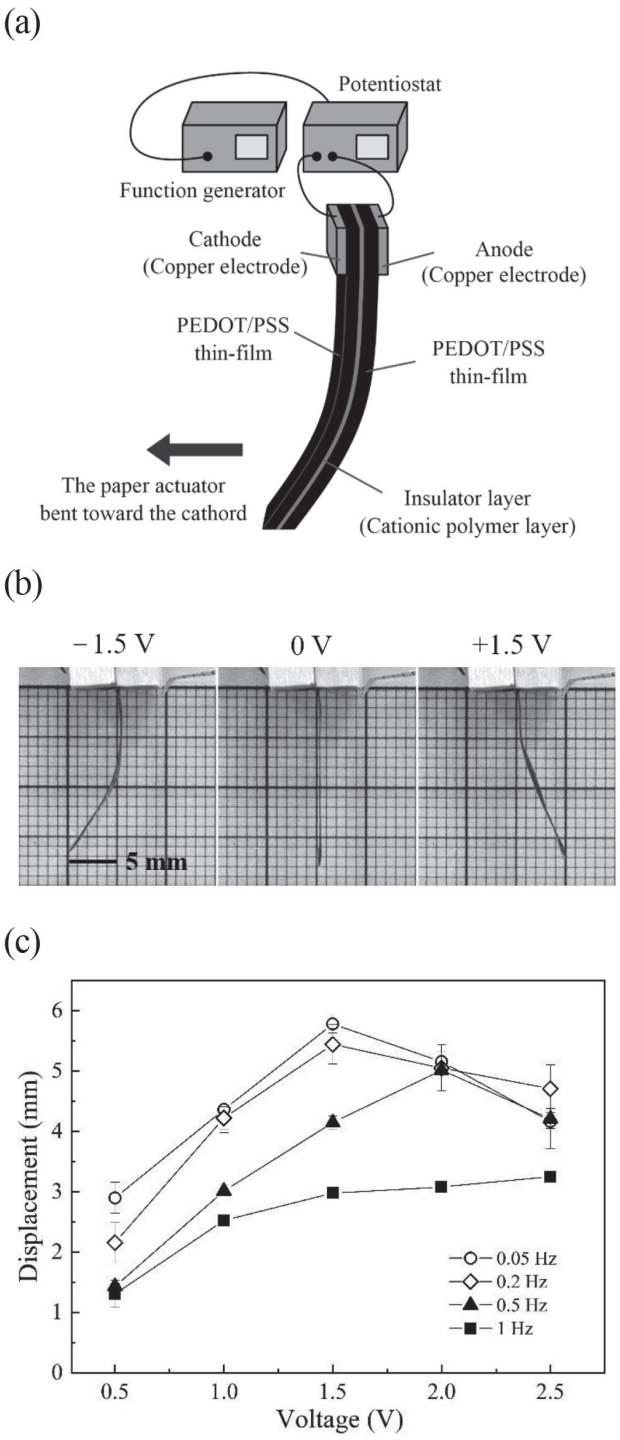

Fig. 3 Actuation properties of the paper actuator with a thickness of 48 μm. (a) Schematic diagram of the actuator operation. (b) Deformations of the paper actuator observed at a square-wave voltage of ±1.5 V and frequency of 0.05 Hz. (c) Average displacements of the paper actuator plotted as functions of the applied voltage at frequencies of 0.05, 0.2, 0.5, and 1 Hz.

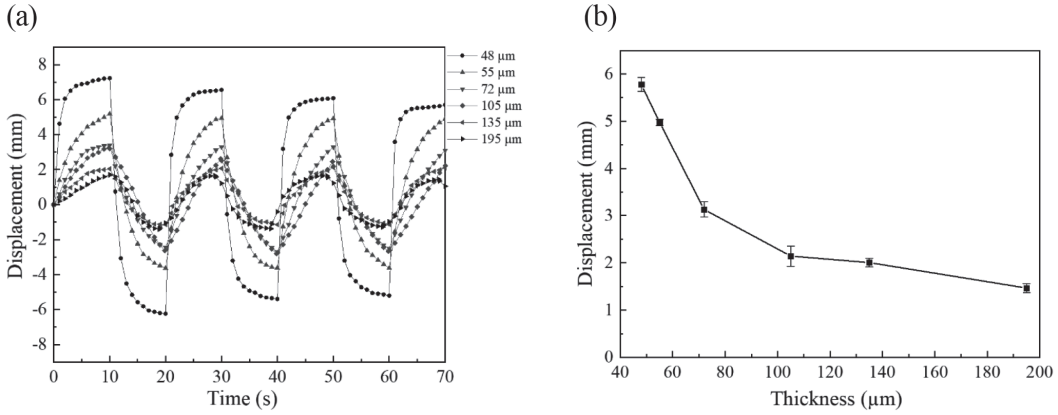

Fig. 4 Actuation properties of the PEDOT/PSS actuators with different actuator thicknesses. (a) Effect of the actuator thickness on the actuator deflection at a square-wave voltage of ±1.5 V and frequency of 0.05 Hz. (b) Average displacements of the paper actuators with different thicknesses measured at a voltage of 1.5 V and frequency of 0.05 Hz.

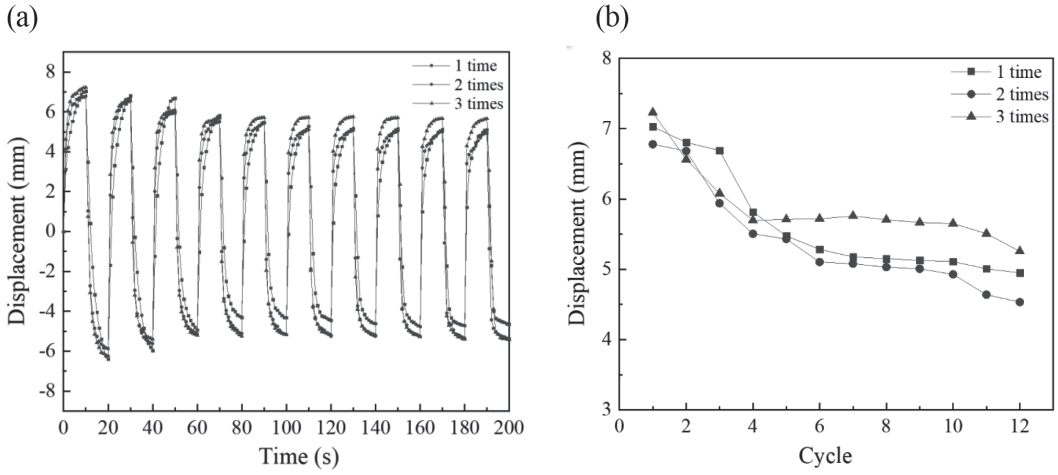

Fig. 5 (a) Reproducibility of the displacements of the paper actuator with a thickness of 48 μm measured at a square-wave voltage of ±1.5 V and frequency of 0.05 Hz. (b) Actuator displacements plotted as functions of the number of cycles.

es of 48–195 μm were prepared to assess the effects of actuator thickness on the actuator response and maximum displacement (Fig. 4).

Figure 4a displays the responses of the PEDOT/PSS actuators with various thicknesses measured at a square-wave voltage of ±1.5 V and frequency of 0.05 Hz. With decreasing the actuator thickness, the peak-to-peak displacement significantly increased. In Fig. 4b, the peak displacement (averaged from the third to eighth cycles) is plotted as a function of the actuator thickness. Among the examined samples, the actuator with a thickness of 48 μm demonstrated the largest displacement (5.8 mm), and the actuator with a thickness of 195 μm exhibited the smallest displacement (1.5 mm). Figure 4a also shows that the initial deformation slope noticeably increased with decreasing thickness, indicating that the thinner actuator deformed more quickly in response to an electric field; a similar effect was observed for IPMCs containing Nafion membranes[20, 26]. Therefore, the thickness/deformability relationship is an important characteristic of both paper actuators and IPMCs.

3.4 Reproducibility of actuator displacement measurements

Figure 5 describes the actuation properties of the PEDOT/PSS actuator as a function of cycles. Three sets of measurements were performed for the paper actuator with a of thickness 48 μm (Fig. 5a). Before each measurement, the actuator was dipped into water, and the excess water was wiped off. Owing to this rehydration procedure, the first cycle of each measurement set produced an almost identical peak displacement (7.0 ± 0.2 mm), and the displacement curves obtained for the three sets of measurements had similar shapes. This observation suggested that

the deflection of the paper actuator exhibited good reproducibility during the repeated cycles.

In Fig. 5b, the maximum peak displacements are plotted as functions of the number of actuation cycles. The obtained plots demonstrated decreases in the peak displacement over the course of 12 cycles due to water evaporation. As shown in section 3.2, the paper actuator performance was strongly influenced by its deformation capability/softness, which was sensitive to the water content. Hence, the rehydration of the actuator before each measurement ensured good reproducibility of its deformations, indicating that the hydration process was critical for the proper actuation of this device.

4 Conclusions

In this study, three-layer paper actuators were prepared by sandwiching a polyelectrolyte layer between two PEDOT/PSS electrode films. The actuation properties of the paper actuator were assessed at various applied voltages and frequencies. The paper actuators demonstrated stable and reproducible actuation characteristics with relatively large deflections and bilateral symmetries. In addition, the actuator displacement increased considerably with reducing actuator thickness. The maximum average displacement of 5.8 mm was achieved for a 48 μm thick actuator at a voltage of 1.5 V and frequency of 0.05 Hz.

Conflicts of Interest

The authors declare no conflict of interest.

References

1) Doufène, K.; Tourné-Péteilh, C.; Etienne, P.; Aubert-Pouëssel, A. Microfluidic systems for droplet generation in aqueous continuous phases: A focus review. *Langmuir* **35**, 12597-12612(2019).
2) Takagi, J.; Yamada, M.; Yasuda, M.; Seki, M. Continuous particle separation in a microchannel having asymmetrically arranged multiple branches. *Lab Chip* **5**, 778-874(2005).
3) Huang, S.H.; Chang, Y.S.; Juang, J.J.; Chang, K.W.; Tsai, M.H.; Lu, T.P.; Lai, L.C.; Chuang, E.Y.; Huang, N.T. An automated microfluidic DNA microarray platform for genetic variant detection in inherited arrhythmic diseases. *Analyst* **143**, 1367-1377(2018).
4) Kolluri, N.; Klapperich, C.M.; Cabodi, M. Towards lab-on-a-chip diagnostics for malaria elimination. *Lab Chip* **18**, 75-94(2017).
5) Feng, J.; Yuan, J.; Cho, S.K. Micropropulsion by an acoustic bubble for navigating microfluidic spaces. *Lab Chip* **15**, 1554-1562(2015).
6) DeMello, A.J. Control and detection of chemical reactions in microfluidic systems. *Nature* **442**, 394-402(2006).
7) Zhang, D.; Bi, H.; Liu, B.; Qiao, L. Detection of pathogenic microorganisms by microfluidics based analytical methods. *Anal. Chem.* **90**, 5512-5520(2018).
8) Kant, K.; Shahbazi, M.A.; Dave, V.P.; Ngo, T.A.; Chidambara, V.A.; Than, L.Q.; Bang, D.D.; Wolff, A. Microfluidic devices for sample preparation and rapid detection of foodborne pathogens. *Biotechnol. Adv.* **36**, 1003-1024(2018).
9) Oeschger, T.; McCloskey, D.; Kopparthy, V.; Singh, A.; Erickson, D. Point of care technologies for sepsis diagnosis and treatment. *Lab Chip* **19**, 728-737(2019).
10) Jung, W.; Han, J.; Choi, J.W.; Ahn, C.H. Point-of-care testing(POCT)diagnostic systems using microfluidic lab-on-a-chip technologies. *Microelectron Eng.* **132**, 46-57(2015).
11) De Volder, M.; Reynaerts, D. Pneumatic and hydraulic microactuators: a review. *J. Micromech. Microeng.* **20**, 043001(2010).
12) Cazorla, P.H.; Fuchs, O.; Cochet, M.; Maubert, S.; Le Rhun, G.; Robert, P.; Fouillet, Y.; Defay, E. Piezoelectric micro-pump with PZT thin film for low consumption microfluidic devices. *Procedia Eng.* **87**, 488-491(2014).
13) Zhao, B.; Cui, X.; Ren, W.; Xu, F.; Liu, M.; Ye, Z.G. A controllable and integrated pump-enabled microfluidic chip and its application in droplets generating. *Sci. Rep.* **7**, 11319(2017).
14) Said, M.M.; Yunas, J.; Bais, B.; Hamzah, A.A.; Majlis, B.Y. The design, fabrication, and testing of an electromagnetic micropump with a matrix-patterned magnetic polymer composite actuator membrane. *Micromachines* **9**, 13(2017).
15) Rahbar, M.; Seyfollahi, S.; Khosla, A.; Gray, B.L.; Shannon, L. Fabrication process for electromagnetic actuators compatible with polymer based microfluidic devices. *ECS Trans.* **41**, 7-17(2012).
16) Yun, J.S.; Yang, K.S.; Choi, N.J.; Lee, H.K.; Moon, S.E.; Kim, D.H. Microvalves based on ionic polymer-metal composites for microfluidic application. *J. Nanosci. Nanotechnol.* **11**, 5975-5979(2011).
17) Nam, D.N.C.; Ahn, K.K. Design of an IPMC diaphragm for micropump application. *Sens. Actuators A* **187**, 174-182(2012).
18) Kim, O.; Kim, S.J.; Park, M.J. Low-voltage-driven soft actuators. *Chem. Commun.* **54**, 4895-4904(2018).
19) Bahramzadeh, Y.; Shahinpoor, M. A review of ionic polymeric soft actuators and sensors. *Soft Robotics* **1**, 38-52(2014).
20) Kim, B.; Kim, B.M.; Ryu, J.; Oh, I.H.; Lee, S.K.; Cha,

S.E.; Pak, J. Analysis of mechanical characteristics of the ionic polymer metal composite (IPMC) actuator using cast ion-exchange film. *Proc. SPIE* **5051**, 486-495 (2003).
21) Wang, H.S.; Cho, J.; Song, D.S.; Jang, J.H.; Jho, J.Y.; Park, J.H. High-performance electroactive polymer actuators based on ultrathick ionic polymer–metal composites with nanodispersed metal electrodes. *ACS Appl. Mater. Interfaces* **9**, 21998-22005 (2017).
22) Hara, Y.; Yamaguchi, Y. Development of a paper actuator with PEDOT: PSS thin-films as an electrode. *Actuators* **3**, 285-292 (2014).
23) Shahinpoor, M.; Kim, K.J. Ionic polymer-metal composites: I. Fundamentals. *Smart Mater. Struct.* **10**, 819-833 (2001).
24) Li, Y.; Tanigawa, R.; Okuzaki, H. Soft and flexible PEDOT/PSS films for applications to soft actuators. *Smart Mater. Struct.* **23**, 074010 (2014).
25) Wang, D.; Lu, C.; Zhao, J.; Han, S.; Wu, M.; Chen, W. High energy conversion efficiency conducting polymer actuators based on PEDOT:PSS/MWCNTs composite electrode. *RSC Adv.* **7**, 31264-31271 (2017).
26) He, Q.; Yu, M.; Song, L.; Ding, H.; Zhang, X.; Dai, Z. Experimental study and model analysis of the performance of IPMC membranes with various thickness. *J. Bionic Eng.* **8**, 77-85 (2011).